

See discussions, stats, and author profiles for this publication at: <https://www.researchgate.net/publication/261597567>

Two Metal–Organic Frameworks with a Tetratopic Linker: Solvent–Dependent Polymorphism and Postsynthetic Bromination

ARTICLE *in* CRYSTAL GROWTH & DESIGN · FEBRUARY 2014

Impact Factor: 4.89 · DOI: 10.1021/cg4018536

CITATIONS

12

READS

96

3 AUTHORS, INCLUDING:



Frank Hoffmann

University of Hamburg

55 PUBLICATIONS 2,629 CITATIONS

[SEE PROFILE](#)



Michael Fröba

University of Hamburg

219 PUBLICATIONS 5,766 CITATIONS

[SEE PROFILE](#)

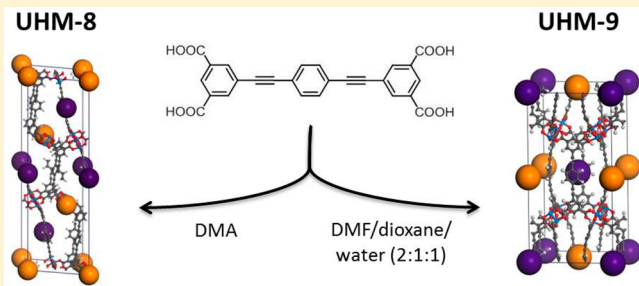
Two Metal–Organic Frameworks with a Tetratopic Linker: Solvent-Dependent Polymorphism and Postsynthetic Bromination

Daniela Frahm, Frank Hoffmann, and Michael Fröba*

Institute of Inorganic and Applied Chemistry, Department of Chemistry, University of Hamburg, Martin-Luther-King-Platz 6, D-20146 Hamburg, Germany

Supporting Information

ABSTRACT: Synthesis of two polymorphous porous metal–organic frameworks (MOFs), both based on a linear tetracarboxylate linker containing ethinyl functionalities and copper ions, is presented. The resulting structure of the MOF is highly dependent on the solvent used during the synthesis: use of *N,N*-dimethylacetamide as a solvent results in a three-dimensional structure with *fof* topology (UHM-8)—a widespread net regarding MOFs composed of linear tetracarboxylates and copper ions—while a solvent mixture of *N,N*-dimethylformamide, dioxane, and water (2:1:1) gives rise to a three-dimensional structure based on the more rare *stx* net (UHM-9). Possible reasons why which topology is favored in each case is discussed in terms of the thermodynamic stability and solvent stabilizing effects. Furthermore, the first postsynthetic modification (PSM) of a nonterminal triple bond inside a MOF structure was accomplished by addition of bromine under mild conditions to UHM-8. Quantitative conversion rates and retention of the crystallinity of the brominated MOF could be confirmed by Raman and NMR spectroscopy and powder X-ray diffraction, respectively.



INTRODUCTION

Although the term polymorphism is widely used in solid-state chemistry, an all-encompassing definition is elusive. The first modern definition, given by McCrone in 1965, reads as follows: “*A polymorph is a solid crystalline phase of a given compound resulting from the possibility of at least two different arrangements of the molecules of that compound in the solid state.*”¹ However, there are some cases, which are not unambiguously covered by this definition, arising mainly from the difficulty to decide always without remaining doubts if “a given compound” is “the same” or “not the same”. This applies, for instance, for tautomers.² Another famous example is the debate on the two proposed forms of aspirin crystals, which was recently fully resolved by Bond, Boese, and Desiraju, who could show that aspirin in some cases crystallizes as a mixture between the two slightly distinct forms even within one single crystal.³ Due to such ambiguities, further terms such as “pseudopolymorphism” (covering, for example, hydrates and solvates) have been established. Unfortunately, this results in further discussions about this issue rather than creating distinctiveness.^{4,5} In any case, polymorphism is a frequently occurring phenomenon in various areas of solid-state chemistry, particularly important in the pharmaceutical industry because polymorphs of the active compound are often known to have a decisive influence on its pharmaceutical properties.⁶ Another large field of solid-state chemistry is given by metal–organic frameworks (MOFs), which constitute a class of hybrid materials composed of inorganic parts like metal ions or metal–oxygen clusters

bridged by organic ligand molecules.^{7–10} These crystalline coordination polymers exhibit manifold properties for a wide variety of applications like gas storage,^{11–13} chemical separation,¹⁴ sensing,^{15,16} magnetism,¹⁷ or catalysis.^{18,19} Due to the enormous variety of building blocks and synthesis parameters influencing the crystal engineering process an almost infinite structural diversity is offered in which also the occurrence of polymorphism is no longer a rarity.^{20–24} In the majority of cases, polymorphism in MOFs is manifested as constituting different topologies. A well-known example is given by the realization of the two different topologies **nbo** and **pts** of MOFs comprising tetracarboxylate linkers. Subtle changes of the synthesis conditions like temperature or duration can lead to the one or the other topology.^{25,26} Furthermore, Chen et al. could show that the cobalt-based MOF-501 (**nbo**) can be postsynthetically converted into the slightly thermodynamically more stable polymorphic form MOF-502 (**pts**) simply by heating.²⁶ In addition to synthesis temperature and duration, often the solvent used plays a decisive and in many cases an unclear and extreme complex role. To date, several instances of solvent-dependent polymorphisms in the area of MOFs are known (not to be confused with the “pseudopolymorphism” of solvates mentioned above).^{27–31} Besides the cases in which different solvents lead

Received: December 12, 2013

Revised: February 13, 2014

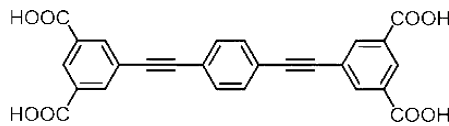
Published: February 19, 2014

to different topologies a particularly interesting case of a symmetry-preserving supramolecular stereoisomerism of the nbo net (called α and β phase) is reported by Zhou and co-workers.³² Understanding the phenomena of polymorphism and the determining parameters of the specific structural formation of the building blocks of a particular MOFs is of vital importance in order to be able to influence the characteristics of the framework, such as pore size or volume, in a desired direction, particularly with regard to special applications.

Apart from controlling the structure-building process in MOFs a further possibility to tune their properties, in particular, in terms of surface polarity or functionalities, is given by postsynthetic modification (PSM).^{33–35} PSM is of great interest due to several reasons: It offers a possibility to include functional groups into the MOF structure by chemical transformation of the organic linker component in the crystalline material, which might not be accessible via the classical solvothermal reaction route. Furthermore, the MOFs could be functionalized in either the interior or the exterior by the choice of the size of the transforming reagent to give a sort of “core–shell MOFs”.³⁶ To date, there are many examples of PSM reactions in MOFs, like the transformation from primary into secondary amines or amides, conversion of aldehydes into imines, the famous “click reaction” between terminal alkynes and azides, as well as halogenation of double bonds.^{36–41} Bauer et al., for instance, presented a diastereoselective heterogeneous bromination of the linker *trans*-4,4'-stilbene dicarboxylate using the PSM approach. Due to the strong ligand coordination to the metal of the MOF, the rotation along the C–C bond during bromination was hindered to a great extent, resulting exclusively in the meso isomer. Another example of postsynthetic bromination of a double bond was shown by Suh et al. in 2012.⁴² The linker of MOF SNU-70 was brominated almost quantitatively at room temperature, giving rise to the new MOF SNU-70Br, thereby retaining the overall structure and porosity. Although many MOFs contain C–C triple bonds, only a very few of them were subjected to PSM reactions. Besides modification of terminal triple bonds, e.g., with the help of “click reactions”, modification of nonterminal triple bonds of MOFs is to the best of our knowledge so far unknown. Introducing bromine functionalities into MOF structures opens the way for further modification reactions and could be beneficial regarding gas adsorption applications due to a higher polarizability of the linker.⁴³

In this work we present the synthesis and characterization of two copper-based MOF structures (UHM-8 and UHM-9) with different topologies constructed from a linear tetratopic linker containing two triple bonds (Scheme 1). They could be

Scheme 1. Constitutional Formula of the Linker 5,5'-(1,4-Phenylenedi-2,1-ethinyl)bis(1,3-benzenedicarboxylic acid)



determined as solvent-dependent polymorphs. Although the first polymorph (UHM-8) has very recently already been published by Zheng et al. as NJU-Bai12, the second polymorph (UHM-9) is not mentioned in their work.⁴⁴ According to McCrone's opinion that “every compound has different polymorphic forms, and that, in general, the number of forms

known for a given compound is proportional to the time and money spent in research on that compound”¹ this system seems not to be analyzed completely yet and has further potential for investigations concerning polymorphism. Additionally, we report on the first postsynthetic modification of a nonterminal triple bond within a MOF by quantitative bromination.

■ EXPERIMENTAL SECTION

The synthesis and characterization of the linker as well as the chemicals and devices used are described in the Supporting Information.

Synthesis of the MOFs. In a typical synthesis 400 mg (0.88 mmol) of the linker (Scheme 1) was dissolved in 15 mL of DMA (for UHM-8) or DMF/dioxane/water (2:1:1, for UHM-9) in a 50 mL flask and heated to 100 °C. Afterward, 400 mg (1.66 mmol) of copper(II) nitrate trihydrate dissolved in 10 mL of DMA (for UHM-8) or DMF/dioxane/water (2:1:1, for UHM-9) containing 5 drops of hydrochloric acid (37%) was added dropwise, and the mixture was stirred at 100 °C for 24 h. The resulting bluish-green precipitate was collected by filtration, washed twice with the solvent used during synthesis, and dried in vacuum.

Bromination of UHM-8. A 30 mg amount of UHM-8 was suspended in 3 mL of amyl acetate containing 10 μ L of bromine and 1 mg of AlBr₃ as a catalyst. After 24 h at room temperature the MOF was washed by replacing the solvent several times by fresh amyl acetate until no further color changing of the solvent could be observed. To analyze the linker after the bromination process, the MOF was suspended in water and the brominated linker was precipitated by adding diluted hydrochloric acid dropwise. The precipitate was filtrated and dried in vacuum.

■ RESULTS AND DISCUSSIONS

Synthesis of UHM-8 and UHM-9. The reaction of the linker (Scheme 1) with copper(II) nitrate is solvent controlled. Synthesis with the solvent DMA at 100 °C leads exclusively to polymorph one (UHM-8), while a solvent mixture of DMF/dioxane/water (2:1:1) resulted solely in polymorph two (UHM-9). Both reactions give rise to bluish-green powders that could be dried in vacuum and are stable in air. Unfortunately, all attempts to activate these two MOFs including thermal activation (100–170 °C), solvent exchange in combination with thermal activation (acetone, methanol/dichloromethane, or ethanol for 1–8 days, 100–120 °C), or extraction with supercritical carbon dioxide (from 1 h to 2 days) failed and resulted in a collapse of the structures. Even applying the identical protocol described by Zheng et al. to activate NJU-12Bai^{43,45} does not lead to the activated structure, for which we have no explanation so far.

PXRD and Structure Modeling. The crystal sizes of the synthesized compounds UHM-8 and UHM-9 were too small in order to carry out single-crystal X-ray diffraction studies. However, the structures of the two MOFs were solved using a combination of molecular modeling techniques in analogy to the procedure described by Loiseau et al.⁴⁶ and experimental powder X-ray diffraction data. Using the structure of MOF-SO5⁴⁷ and NOTT-109⁴⁸ as starting points the structures of UHM-8 and UHM-9, respectively, were modeled. In the first step the linker molecules were substituted by the new linker (Scheme 1). After removing any symmetry restrictions the constructed model was submitted to a full energy minimization, including optimization of the unit cell, applying the force-field UFF as implemented in the Material Studio v4.4⁴⁹ package. This energy minimization procedure resulted in a plausible trigonal structure with the space group $R\bar{3}$ for UHM-8 ($a = b = 18.62 \text{ \AA}$, $c = 54.44 \text{ \AA}$, $\alpha = \beta = 90.0^\circ$, $\gamma = 120.0^\circ$, $V = 16\,342 \text{ \AA}^3$)

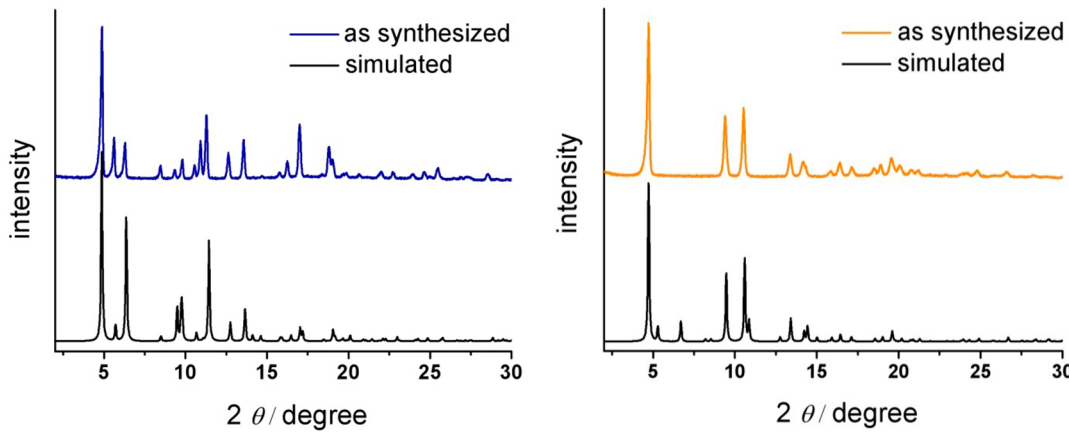


Figure 1. Experimental and simulated powder X-ray diffractograms of UHM-8 (left) and UHM-9 (right).

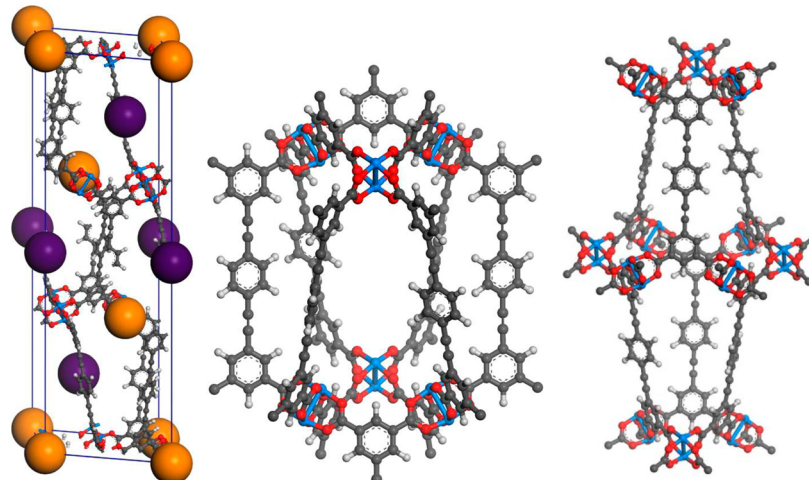


Figure 2. Unit cell (left) of UHM-8 with an oblique view, and visualization of the positions of the two different pore types within the structure: violet spheres represent the position of pore I, and orange spheres show the position of pore II. Isolated pores are shown in the middle (pore I) and on the right (pore II): gray, carbon; red, oxygen; blue, copper; white, hydrogen.

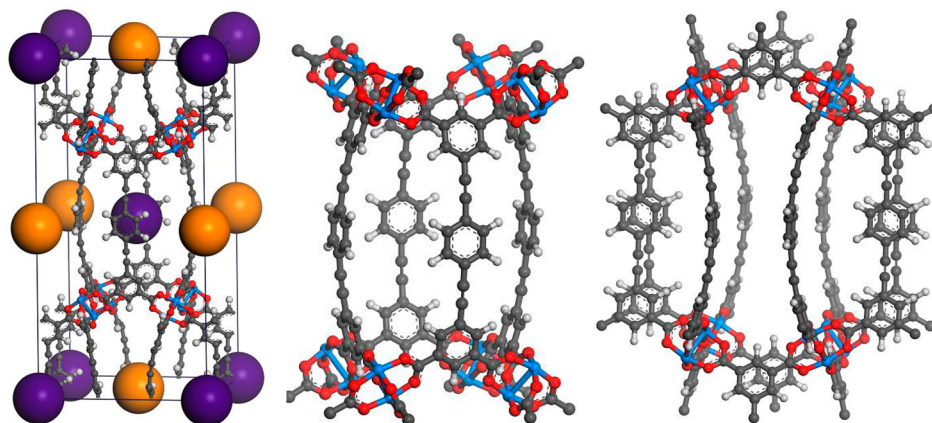


Figure 3. Unit cell of UHM-9 with an oblique view, and visualization of the position of the two different pore types within the structure (left): violet and orange spheres represent the position of pores I and II, respectively. Isolated two pores are shown in the middle (pore I) and on the right (pore II): gray, carbon; red, oxygen; blue, copper; white, hydrogen.

and a tetragonal structure with the space group $I4/mmm$ for UHM-9 ($a = b = 18.65 \text{ \AA}$, $c = 37.34 \text{ \AA}$, $\alpha = \beta = \gamma = 90.0^\circ$, $V = 12\,982 \text{ \AA}^3$). In Figure 1 the experimental and simulated PXRD patterns are compared. Besides some differences concerning the intensity ratio of some of the reflections the simulated and

experimental patterns are in good agreement, allowing validating both structural models. Additional reflections in the simulated pattern of UHM-9 ($2\Theta = 5.3^\circ$, 6.7° , and 10.9°) that are not visible in the respective experimental pattern (Figure 1, right) can probably be attributed to the fact that solvent

molecules were not accounted for in the structural model. For UHM-8 the experimental pattern shows only one additional reflex ($2\Theta = 10.9^\circ$), which is absent in simulated PXRD (Figure 1, left), for which we have no explanation. However, it is interesting to note that the simulated PXRD of the single-crystal data of NJU-Bai12—whose structure is identical to the model we proposed for UHM-8—shows exactly the same PXRD, including this reflection at $10.9^\circ 2\Theta$.⁴⁴

Structural Description. The structure of UHM-8 consists of square-planar four-connected dicopper paddle wheel units bridged by the four-connected linker that could also be described as a square-planar node, because the four carboxylate groups are almost coplanar. The structure can be described by the combination of two different pores: The first pore (Figure 2, middle), comprised of 6 copper paddle wheel motifs and 6 linkers, has a dimension of about $11 \times 13 \text{ \AA}$, while the second pore (Figure 2, right) is bordered by 12 copper paddle wheel motifs and 6 linkers and has a considerably elongated shape with dimensions of $11 \times 31 \text{ \AA}$. The two pores are connected via joint triangular windows built of three copper paddle wheels, giving rise to a hexagonal channel structure along the c axis. The channels are connected in turn again through triangular windows, which are in this case built of two joint linkers and three joint paddle wheels. The unit cell illustrating the positions of the two different pores (violet, pore I; orange, pore II) is shown in Figure 2 (left).

The building units of the framework of UHM-9 are the same as in UHM-8; however, the connection scheme is different, resulting in a different net, too. Pore type I (Figure 3, middle) is constructed by eight paddle wheel motifs and four linkers and has dimensions of $9 \times 13 \text{ \AA}$, while pore type II is bordered by eight paddle wheel motifs and eight linkers (Figure 3, right) and has dimensions of $11 \times 13 \text{ \AA}$. Unlike in UHM-8, the two pore types are connected along the c axis via windows built up of four paddle wheels and along the a and b axes via two shared linker molecules and two paddle wheels. The unit cell along with the location of the two pore types is shown in Figure 3 (left). In contrast to the structure of UHM-8, in which the linker adopts an almost planar conformation, the linker in UHM-9 is considerably bent by approximately 20° . The phenomenon of bent linkers is already known in the literature, in particular, for linkers with *p*-(phenyleneethynylene) units as, for instance, incorporated into MOFs belonging to the PIZOF series of Behrens and co-workers.^{50–52}

Topological Analysis. The topology of MOFs being isostructural or isoreticular to UHM-8 and UHM-9 are already known in the literature and were frequently described as 4-connected (4-c) nets with the RCSR⁵³ symbols **nbo** and **pts**, respectively. This analysis is based on the consideration that both the copper paddle wheel motif and the linker represent a 4-c node. However, as pointed out very recently in a very comprehensive review article on this subject,⁵⁴ it is more reasonable to describe the linker as two 3-c nodes. In this way the resulting (3,4)-c net can be regarded as derived from the basic 4-c net. The advantages are 3-fold: (1) one can distinguish between different possibilities for the derived nets that often have the same symmetry; (2) knowledge of the basic net is kept, (3) it gives a better reflection of the coordination geometry and connection scheme. Therefore, the topologies of UHM-8 and UHM-9—analyzed with the help of TOPOS 4.0⁵⁵—should be described more properly as **fof** and **stx** (Systre net with the number 3895 of the EPINET database⁵⁶) nets rather than **nbo** and **pts**, respectively. The presentation of

the two (3,4)-c nets is shown in Figure 4 whereby the blue (4-c) node represents the copper paddle wheel motif and two

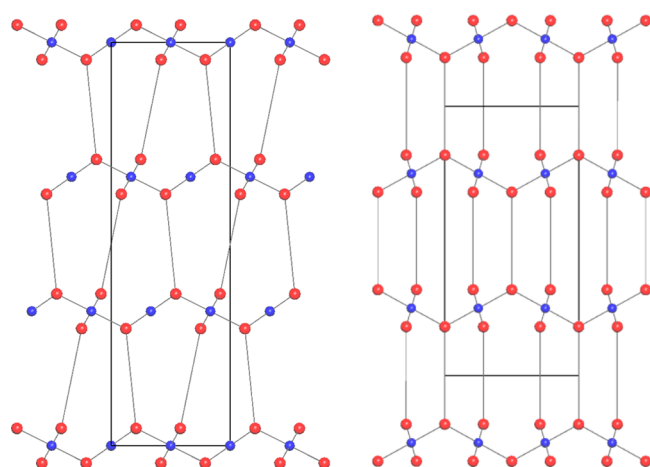


Figure 4. Node representation of the topology of UHM-8 (left, **fof** net) and UHM-9 (right, **stx** net). A blue node represents the copper paddle wheel motif, and two neighboring red nodes represent a linker molecule.

neighboring red (3-c) nodes represent one linker molecule. Figures 5 and 6 show the two topologies in the form of their natural tiling.

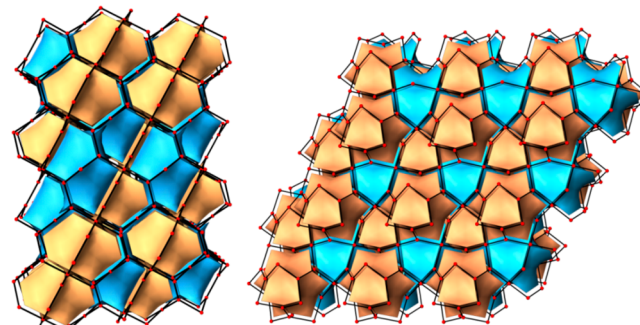


Figure 5. Natural tiling of the **fof** net of UHM-8 viewed along the a axis (left) and c axis (right).

Polymorphism. As already mentioned in the Introduction, the polymorphism of MOFs is an interesting field of research whose occurrence could have different reasons. The two MOFs UHM-8 and UHM-9 constitute an example for solvent-dependent polymorphism of MOFs consisting of linear

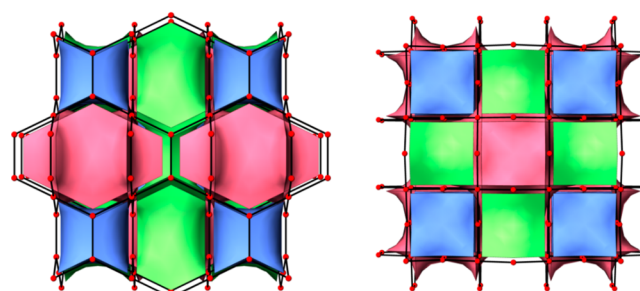


Figure 6. Natural tiling of the **stx** net of UHM-9 with a view along the a axis (left) and c axis (right).

tetracarboxylates and copper ions. Depending on the solvent used during synthesis (DMA or a mixture of DMF/dioxane/water (2:1:1), respectively) formation of either the **fof** or the **stx** net is favored. Taking into account that all other synthesis parameters are the same, the polymorphism is probably based on the different solvent molecules, which offer the possibility to coordinate to the open metal sites during the synthesis process. Therefore, the solvent molecules could have structure-directing properties influencing the resulting MOF structure, a phenomenon of which is already known from the literature.^{27–31} Strictly speaking, two structures with different solvent molecules coordinated to their open metal sites exhibit different compositions and hence are not genuine polymorphs. However, apart from that issue they can be at least regarded as supramolecular isomers.

Regarding MOFs, which are constructed of linear tetracarboxylates and copper ions, formation of a **fof** net is not very surprising as the literature is full of analogous frameworks, see, for instance, the MOF series NOTT-100–NOTT-109, published by the group of Schröder, in which 9 of 10 linear tetracarboxylates give rise to MOF structures exhibiting **fof** topology.⁵⁷ Only NOTT-109 is different by forming the **stx**⁵⁷ net. This was explained by the bulky central naphthalene bridge of the linker, preventing formation of the triangular window being part of the **fof** topology.⁵⁸ However, tetracarboxylate linkers with bridges even bulkier—like anthracene—give rise to formation of the **fof**⁵⁷ net again as exemplified in PCN-14 by the group of Zhou.⁵⁹ Thus, there must be other reasons that are responsible for formation of the one or the other network.

Taking a closer look at the structures of UHM-8 and UHM-9 reveals the difference of these two topologies and could possibly give an explanation for the preference of the **fof** topology. Although both nets are (3,4)-c, the regional environment of the two neighboring 3-c nodes is different for the two MOFs. The linker in the structure of UHM-8 is sigmoidal shaped, and the linker of UHM-9 is rather u-shaped (see Figure 7, top). Therefore, the connection of the 3-c (red) nodes to the 4-c (blue) nodes lies on different sides of an

imaginary plane running through the two neighboring 3-c nodes in the case of UHM-8 (**fof**), while these connections are located on the same side of this plane in the case of UHM-9 (**stx**) (see Figure 7, bottom). Due to the fact that the linker in the **stx** topology is bent more strongly in absolute terms (approximately by 20°), the building process of MOF structures with **fof** topology is possibly favored.

UHM-8 and UHM-9 are the two polymorphs of the copper ion/linker system at hand, which could be fully resolved. However, we experienced by exploration of the synthesis parameter field that there are at least three further different phases. Unfortunately, the exact structure of these three crystalline phases (I, II, and III; all in the form of bluish-green powders) could not be solved yet. Considering that they are composed of the same components as UHM-8 and UHM-9 they could be either further polymorphs of UHM-8 and UHM-9 or pseudopolymorphs differing in, e.g., the SBU; in principle, also nonpolymorphs like chain-like polymers are conceivable. The corresponding PXRDs are shown in Figure S3 (see Supporting Information). Phase I was obtained by synthesis in the same solvent mixture as in the case of UHM-9 (DMF/dioxane/water (2:1:1) plus 5 drops of HCl); however, it was carried out in a microwave (200 W, 30 min) instead of using a flask heated up to 100 °C. Synthesis of phase II was also carried out in a microwave (again 200 W, 30 min) with the mentioned solvent mixture, but here 5 drops of HNO₃ instead of HCl were added. Finally, changing the solvent mixture from DMF/dioxane/water (2:1:1) to DMF/ethanol/water (3:3:2) (without any addition of acid) and carrying out the synthesis in an autoclave (80 °C, 24 h) gives rise to phase III. In conclusion, 5 different phases (of which two are real polymorphs) of only one metal ion/linker combination could be generated by changing the synthesis conditions only very slightly, emphasizing the complexity of the framework construction process. The parameters, which might direct the synthesis to a desired product, is far from being completely understood yet. Therefore, we would like to point out that intentional attributes in the area of MOF synthesis—such as “framework design”, “tailoring of properties”, etc.—should be used with great care only.

Postsynthetic Bromination of UHM-8. As described in the Experimental Section, UHM-8 could be brominated almost quantitatively in a postsynthetic modification reaction, giving UHM-8-Br (Figure 8).

The PXRD pattern of UHM-8-Br shows a high degree of crystallinity and good agreement with the respective simulated PXRD pattern (Figure 9). Furthermore, the reaction progress of the bromination reaction could be monitored by Raman spectroscopy (Figure 10). The band at 2214 cm⁻¹, typical of the stretching vibration of alkynes, decreases with increasing reaction time. After 24 h this band almost vanished. In turn, a band at 1628 cm⁻¹ appeared, typical of stretching vibrations of double bonds in conjugation with aromatic rings. In addition, with increasing reaction time, a band at 500 cm⁻¹ evolved, which can be tentatively assigned to the C–Br stretching vibration.

After the bromination reaction the linker of the MOF was isolated and identified by NMR spectroscopy (see Supporting Information, S4–S7).

To the best of our knowledge, the postsynthetic modification of UHM-8 is the first modification of a nonterminal triple bond within a MOF. The triple bonds within the linker were converted into a more advantageous function that could be

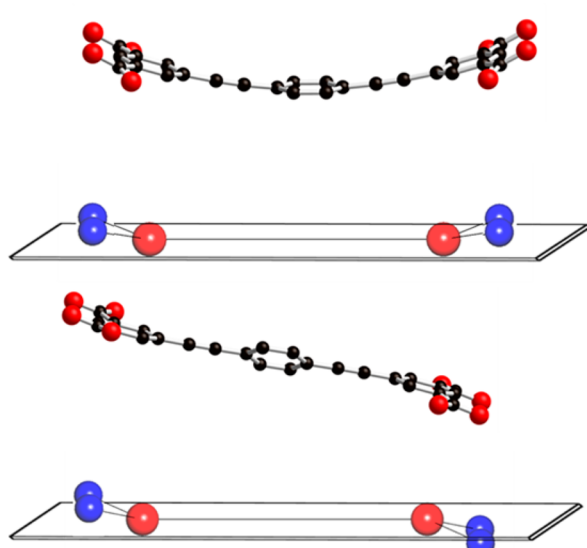


Figure 7. Linker in the structure of UHM-8 (top, right) and UHM-9 (top, left) as well as the respective part of the **fof** net (bottom, right) and **stx** (bottom, left) in node representation (right).

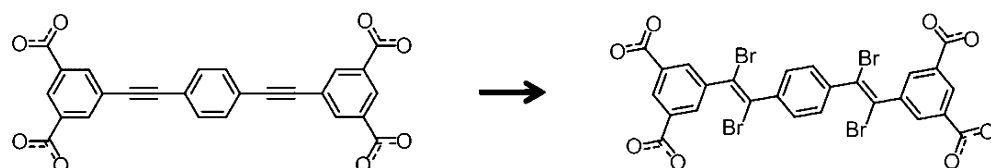


Figure 8. Linker of UHM-8 before (left) and after bromination (right).

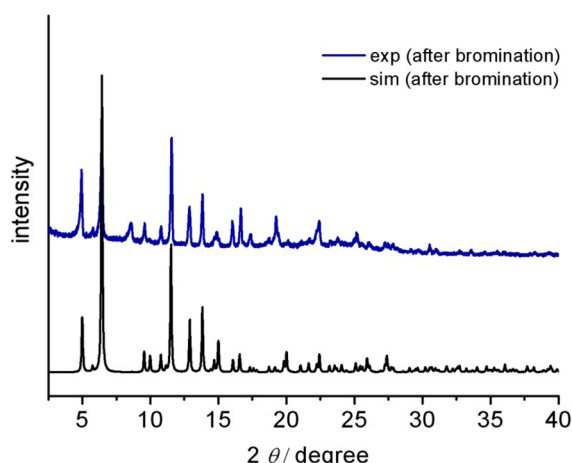


Figure 9. Experimental (blue) and simulated (black) PXRD pattern of brominated UHM-8 (UHM-8-Br).

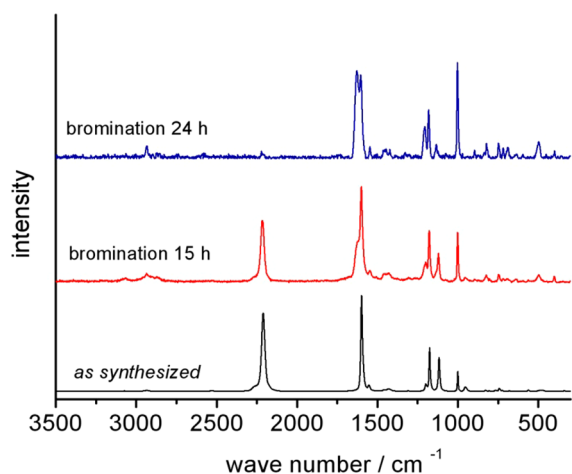


Figure 10. Bromination progress as monitored by Raman spectra: pure UHM-8 (as synthesized, black) and after 15 h (red) as well as 24 h bromination time (blue).

used for further functionalization of the MOF compound for specific applications. Furthermore, integration of the bromine substituents could have a beneficial influence on gas adsorption applications due to a higher polarizability of the linker.⁴³ Corresponding investigations are under way.

CONCLUSIONS

This work presents the synthesis and characterization of two polymorphic copper-based MOFs, UHM-8 and UHM-9, containing tetracarboxylate 5,5'-(1,4-phenylenedi-2,1-ethinyl)-bis(1,3-benzenedicarboxylic acid) as a linker. The structure of the final product can be influenced by the choice of solvent. Use of DMA leads to formation of UHM-8 having **fof** topology and using DMF/dioxane/water (2:1:1) results in the structure of UHM-9 forming a **stx** net. The fact that the majority of

MOFs composed of copper ions and linear tetracarboxylates favorably realize the **fof** net was explained on the basis of the linker structure *inside* the MOF. The appearance of three further phases containing the same components as UHM-8 and UHM-9 by only small variations of the synthesis conditions reflects the responsibility of MOF synthesizes in general. Finally, with successful quantitative bromination of UHM-8, the first modification of a nonterminal triple bond within a MOF was accomplished.

ASSOCIATED CONTENT

Supporting Information

Synthesis of the linker, TG/DTA/MS data of the MOFs, model structures of UHM-8 and UHM-9 as CIFs, PXRDs of further phases and ¹H and ¹³C NMR data of the brominated and unbrominated linker. This material is available free of charge via the Internet at <http://pubs.acs.org>.

AUTHOR INFORMATION

Corresponding Author

*Phone +49-40-42838-3100. Fax: +49-40-42838-6348. E-mail: michael.froeba@chemie.uni-hamburg.de.

Notes

The authors declare no competing financial interest.

ACKNOWLEDGMENTS

D.F. thanks the Graduate School for Resource and Energy Management 'C1-REM' (Excellence Initiative of the Federal State Hamburg) for financial support.

REFERENCES

- (1) McCrone, W. C. In *Physics and Chemistry of the Organic Solid State*; Fox, D., Labes, M. M., Weissberger, A., Eds.; Interscience Publishers: London, 1965; Vol. 2, pp 725–767.
- (2) Desiraju, G. R. *Cryst. Growth Des.* **2008**, *8*, 3–5.
- (3) Bond, A. D.; Boese, R.; Desiraju, G. R. *Angew. Chem., Int. Ed.* **2007**, *46*, 618–622.
- (4) Bernstein, J. *Polymorphism in Molecular Crystals*; Oxford University Press: New York, 2002.
- (5) Bernstein, J. *Cryst. Growth Des.* **2011**, *11*, 632–650.
- (6) Hilfiker, R. *Polymorphism: In the Pharmaceutical Industry*; Wiley VCH Verlag GmbH & Co.: Weinheim, Germany, 2006.
- (7) James, S. L. *Chem. Soc. Rev.* **2003**, *32*, 276–288.
- (8) Ferey, G. *Chem. Soc. Rev.* **2008**, *37*, 191–214.
- (9) Kaskel, S. *Chem. Ing. Tech.* **2010**, *82*, 1019–1023.
- (10) Stock, N.; Biswas, S. *Chem. Rev.* **2012**, *112*, 933–969.
- (11) Morris, R. E.; Wheatley, P. S. *Angew. Chem.* **2008**, *120*, 5044–5059.
- (12) Suh, M. P.; Park, H. J.; Prasad, T. K.; Lim, D.-W. *Chem. Rev.* **2012**, *112*, 782–835.
- (13) Ma, S. *Pure Appl. Chem.* **2009**, *81*, 2235–2251.
- (14) Li, J.-R.; Sculley, J.; Zhou, H.-C. *Chem. Rev.* **2012**, *112*, 869–932.
- (15) Kreno, L. E.; Leong, K.; Farha, O. K.; Allendorf, M.; Van Duyne, R. P.; Hupp, J. T. *Chem. Rev.* **2012**, *112*, 1105–1125.

- (16) Cui, Y.; Yue, Y.; Qian, G.; Chen, B. *Chem. Rev.* **2012**, *112*, 1126–1162.
- (17) Kurmoo, M. *Chem. Soc. Rev.* **2009**, *38*, 1353–1379.
- (18) Farrusseng, D.; Aguado, S.; Pinel, C. *Angew. Chem.* **2009**, *121*, 7638–7649.
- (19) Lee, J.; Farha, O. K.; Roberts, J.; Scheidt, K. A.; Nguyen, S. T.; Hupp, J. T. *Chem. Soc. Rev.* **2009**, *38*, 1450–1459.
- (20) Gandara, F.; de la Pena-O'Shea, V. A.; Illas, F.; Snejko, N.; Proserpio, D. M.; Gutierrez-Puebla, E.; Angeles Monge, M. *Inorg. Chem.* **2009**, *48*, 4707–4713.
- (21) Liu, G.-X.; Xu, H.; Zhou, H.; Nishihara, S.; Ren, X.-M. *CrystEngComm* **2012**, *14*, 1856–1864.
- (22) Du, M.; Zhao, X.-J.; Guo, J.-H.; Batten, S. R. *Chem. Commun.* **2005**, 4836–4838.
- (23) Liu, G.-X.; Xu, H.; Zhou, H.; Nishihara, S.; Ren, X.-M. *CrystEngComm* **2012**, *14*, 1856–1864.
- (24) Bon, V.; Senkovska, I.; Baburin, I. A.; Kaskel, S. *Cryst. Growth Des.* **2013**, *13*, 1231–1237.
- (25) Sun, D.; Ke, Y.; Mattox, T. M.; Ooro, B. A.; Zhou, H.-C. *Chem. Commun.* **2005**, 5447–5449.
- (26) Chen, B.; Ockwig, N. W.; Fronczeak, F. R.; Contreras, D. S.; Yaghi, O. M. *Inorg. Chem.* **2005**, *44*, 181–183.
- (27) Li, C.-P.; Du, M. *Chem. Commun.* **2011**, *47*, 5958–5972.
- (28) Zhao, X.; Zhang, L.; Ma, H.; Sun, D.; Wang, D.; Feng, S.; Sun, D. *RSC Adv.* **2012**, *2*, 5543–5549.
- (29) Chen, X.-D.; Du, M.; Mak, T. C. W. *Chem. Commun.* **2005**, 4417–4419.
- (30) Dong, W.-W.; Li, D.-S.; Zhao, J.; Ma, L.-F.; Wu, Y.-P.; Duan, Y.-P. *CrystEngComm* **2013**, *15*, 5412–5415.
- (31) Caskey, S. R.; Wong-Foy, A. G.; Matzger, A. J. *Inorg. Chem.* **2008**, *47*, 7751–7756.
- (32) Sun, D.; Ma, S.; Simmons, J. M.; Li, J.-R.; Yuana, D.; Zhou, H.-C. *Chem. Commun.* **2010**, *46*, 1329–1331.
- (33) Cohen, S. M. *Chem. Sci.* **2010**, *1*, 32–36.
- (34) Tanabe, K. K.; Cohen, S. M. *Chem. Soc. Rev.* **2011**, *40*, 498–519.
- (35) Taylor-Pashow, K. M. L.; Della Rocca, J.; Xie, Z.; Tran, S.; Lin, W. *J. Am. Chem. Soc.* **2009**, *131*, 14261–14263.
- (36) Gadzikwa, T.; Farha, O. K.; Malliakas, C. D.; Kanatzidis, M. G.; Hupp, J. T.; Nguyen, S. T. *J. Am. Chem. Soc.* **2009**, *131*, 13613–13615.
- (37) Bzrrows, A. D.; Keenan, L. L. *CrystEngComm* **2012**, *14*, 4112–4114.
- (38) Peikert, K.; Hoffmann, F.; Fröba, M. *Chem. Commun.* **2012**, *48*, 11196–11198.
- (39) Liu, C.; Li, T.; Rosi, N. L. *J. Am. Chem. Soc.* **2012**, *134*, 18886–18888.
- (40) Roy, P.; Schaate, A.; Behrens, P.; Godt, A. *Chem.—Eur. J.* **2012**, *18*, 6979–6985.
- (41) Jones, S. C.; Bauer, C. A. *J. Am. Chem. Soc.* **2009**, *131*, 12516–12517.
- (42) Prasad, T. K.; Suh, M. P. *Chem.—Eur. J.* **2012**, *18*, 8673–8680.
- (43) Sagara, T.; Klassen, J.; Ortony, J.; Ganz, E. *J. Chem. Phys.* **2005**, *123*, 014701.
- (44) Zheng, B.; Yun, R.; Bai, J.; Lu, Z.; Du, L.; Li, Y. *Inorg. Chem.* **2013**, *52*, 2823–2829.
- (45) Following the protocol of activating NJU-Bai12 we soaked as-synthesized samples of UHM-8 and UHM-9 in anhydrous acetone for 3 days to remove the noncoordinated solvent molecules. During that time the solvent was refreshed six times. Afterward, the acetone was removed and the acetone-exchanged sample was dried under a dynamic vacuum at room temperature for 12 h.
- (46) Loiseau, T.; Mellot Draznieks, C.; Muguerza, H.; Ferey, G.; Haouas, M.; Taulelle, F. *C. R. Chim.* **2005**, *8*, 765–772.
- (47) Chen, B.; Ockwig, N. W.; Millward, A. R.; Contreras, D. S.; Yaghi, O. M. *Angew. Chem.* **2005**, *117*, 4823–4827.
- (48) Lin, X.; Telepeni, I.; Blake, A. J.; Dailly, A.; Brown, C. M.; Simmons, J. M.; Zoppi, M.; Walker, G. S.; Thomas, K. M.; Mays, T. J.; Hubberstey, P.; Champness, N. R.; Schroeder, M. *J. Am. Chem. Soc.* **2009**, *131*, 2159–2171.
- (49) Material Studio, v4.4; Accelrys Inc.: San Diego, CA, 2010.
- (50) Schaate, A.; Roy, P.; Godt, A.; Lippke, J.; Waltz, F.; Wiebcke, M.; Behrens, P. *Chem.—Eur. J.* **2011**, *17*, 9320–9325.
- (51) Schaate, A.; Roy, P.; Preuß, T.; Lohmeier, S. J.; Godt, A.; Behrens, P. *Chem.—Eur. J.* **2011**, *17*, 6643–6651.
- (52) Godt, A.; Schulte, M.; Zimmermann, H.; Jeschke, G. *Angew. Chem.* **2006**, *118*, 7722–7726.
- (53) O'Keeffe, M.; Peskov, M. A.; Ramsden, S. J.; Yaghi, O. M. *Acc. Chem. Res.* **2008**, *41*, 1782–1789.
- (54) Li, M.; Li, D.; O'Keeffe, M.; Yaghi, O. M. *Chem. Rev.* **2013**, DOI: 10.1021/cr400392k.
- (55) Blatov, V. A. *Struct. Chem.* **2012**, *23*, 955.
- (56) Ramsden, S. J.; Robins, V.; Hyde, S. T. *Acta Crystallogr., Sect. A* **2009**, *65*, 81–108, <http://epinet.anu.edu.au/>.
- (57) In the original publication the topologies of the MOFs NOTT-100–NOTT-108 were determined as nbo, while NOTT-109 was described as pts net. As already pointed out, these structures should be described as fof and stx net, respectively.
- (58) Lin, X.; Telepeni, I.; Blake, A. J.; Dailly, A.; Brown, C. M.; Simmons, J. M.; Zoppi, M.; Walker, G. S.; Thomas, K. M.; Mays, T. J.; Hubberstey, P.; Champness, N. R.; Schroeder, M. *J. Am. Chem. Soc.* **2009**, *131*, 2159–2171.
- (59) Ma, S.; Sun, D.; Simmons, J. M.; Collier, C. D.; Yuan, D.; Zhou, H.-C. *J. Am. Chem. Soc.* **2008**, *130*, 1012–1016.